

Journal of Rehabilitation in Civil Engineering

Journal homepage: https://civiljournal.semnan.ac.ir/

Extended Hypolastic Model to Measure Geocell Pullout Behavior in Frozen Soil

Ali Namaei-kohal ¹; Alireza Ardakani ^{2,*}

- 1. Postdoctoral Researcher, Department of Civil Engineering, Imam Khmoeini International University, Qazvin, Iran
- 2. Associate Professor, Department of Civil Engineering, Imam Khmoeini International University, Qazvin, Iran
- * Corresponding author: a.ardakani@eng.ikiu.ac.ir

ARTICLE INFO

Article history:

Received: 26 April 2025 Revised: 29 July 2025 Accepted: 17 August 2025

Keywords:

Geosynthetics;

Pullout;

Hypoplastic;

Sand:

Finite Element.

ABSTRACT

This study develops an extended hypoplastic constitutive model to investigate the pullout behavior of geocell-reinforced 131 Sand under freeze-thaw (FT) cycles, addressing the complex mechanical response of frozen soils in cold regions. By incorporating temperature-dependent parameters, intergranular strain effects, and ice formation mechanisms, the model captures nonlinear stressstrain behavior and thermal influences on soil-geocell interaction. Validated through drained triaxial compression tests at -10°C and confining pressures of 100 and 200 kPa, the model accurately predicts stress-strain and volumetric responses. Numerical simulations in Plaxis 3D reveal a 78% increase in pullout resistance in frozen conditions (21.2 kN) compared to unfrozen conditions (11.9 kN) under 20 kPa surcharge, attributed to enhanced ice bonding and interface shear strength. However, repeated FT cycles reduce pullout capacity by approximately 15% after three cycles due to microstructural degradation and weakened confinement. These findings highlight the model's robustness in performance under simulating geocell cyclic thermal offering valuable insights for designing resilient infrastructure in frost-susceptible environments.

E-ISSN: 2345-4423

© 2025 The Authors. Journal of Rehabilitation in Civil Engineering published by Semnan University Press. This is an open access article under the CC-BY 4.0 license. (https://creativecommons.org/licenses/by/4.0/)

How to cite this article:

Namaei-Kohal, A. and Ardakani, A. (2026). Extended Hypolastic model to measure Geocell pullout behavior in frozen soil. Journal of Rehabilitation in Civil Engineering, 14(2), 2324 https://doi.org/10.22075/jrce.2025.2324

1. Introduction

Soil constitutive models are essential for advancing geotechnical engineering, enabling accurate predictions of soil structure performance under various environmental and loading conditions. These models support numerical simulations for designing structures like retaining walls and reinforced slopes. Traditional models, such as Mohr-Coulomb, Cam-Clay, elasto-plastic, and hardening plasticity, provide a foundation for understanding soil behavior. However, they often fail to capture the complex behavior of frozen soils, especially under repeated freeze-thaw (FT) cycles common in cold and permafrost regions.

Freeze-thaw cycles significantly alter soil properties, affecting strength, stiffness, volume, and structure. Li et al. [1] identified four key traits of frozen soils: (1) strong temperature dependency, (2) notable time-dependent behavior, (3) volume expansion from water freezing, and (4) high heterogeneity and anisotropy. These factors make soil behavior more complex, necessitating advanced constitutive models to accurately capture their effects. Several extensions to classical models have been developed. For example, Nishimura et al. [2] enhanced the Cam-Clay model by including temperature and porosity in the effective stress framework, allowing it to address both frozen and unfrozen soils effectively. Yang et al. [3] introduced an elasto-plastic model with a hyperbolic hardening law validated by frozen silt triaxial tests.

Viscoplastic models have proven effective for modeling the rate-dependent and creep behavior of frozen soils, driven by the viscosity of ice and unfrozen water. Yao et al. [4] highlighted the value of viscoplastic formulations, while Hou et al. [5] and Li et al. [6] developed fractional derivative models to simulate complex creep behavior in frozen clay. He et al. [7] further advanced this field through a composite creep model rooted in homogenization theory, effectively bridging micro- and macro-scale deformation responses.

Despite progress, traditional elasto- and visco-plastic models often fail to fully capture frozen soil behavior, especially under cyclic or dynamic loading. The hypoplastic soil model provides a promising alternative with its incremental, non-linear framework, which avoids predefined yield surfaces. It effectively models the transition between elastic and plastic responses, accounting for key factors like density dependency, loading direction, strain accumulation, and intergranular effects, which are crucial for simulating freeze-thaw-induced degradation and recovery in soil behavior.

Xu et al. [8,9] developed a temperature-dependent hypoplastic model for frozen soils, incorporating strain-softening and cohesion as temperature-sensitive factors. However, its limitations in accurately modeling behavior near the freezing point and neglecting internal structural changes in frozen soils indicate a need for further refinement. Subsequent models by Xu et al. [10] introduced rate-dependency and long-term creep simulations, providing better predictions under sustained loads but still lacking in terms of dynamic load simulation capabilities. These capabilities are especially useful in cold-region geotechnics, where soils are repeatedly subjected to thermal and mechanical cycles. Recent applications of this model, including those by Mohammadi and Ardakani, [11,12] have shown promising results in representing soil degradation and recovery due to environmental cycling.

Geosynthetics, especially geocells, have become a practical solution for improving slope stability in both temperate and cold regions. Geocells, three-dimensional polymeric structures, confine soil through frictional and passive resistance, enhancing shear strength and reducing deformations. Their bending stiffness also allows them to distribute stresses effectively, acting as supportive mattresses [13].

The interaction between geocells and surrounding soil is crucial for the stability of reinforced slopes, especially under dynamic or cyclic loading. Numerous studies have explored this interaction. Khedkar and Mandal [14] demonstrated that increasing geocell height improves interaction resistance up to an optimal point. Biabani et al. [15] and Tavakoli and Motarjemi [16] emphasized the role of soil properties,

such as overburden pressure and grain size, in influencing geocell performance. Fakharian and Pilban [17] showed that enhanced geocells offer better bearing capacity and pullout resistance compared to conventional ones, particularly under high-stress conditions.

The influence of freeze-thaw cycles on geocell performance is an emerging area of interest. Namaei-Kohal et al. [18] examined the cyclic and post-cyclic interaction behavior of geocells, revealing how cyclic degradation can compromise the integrity of the geocell-soil interface. Freeze-thaw cycles in frozen environments significantly affect soil mechanical properties and the geosynthetic-soil bond, making their behavior critical. Li et al. [19] and Cui et al. [20] noted that geosynthetics perform well under freezing conditions, but a robust numerical framework is still needed to accurately simulate their behavior in frozen environments. The usage of suitable numerical framework in geotechnical engineering have been widely increased [21–24]

Hypoplastic modeling is highly effective for incorporating temperature effects and strain evolution, making it ideal for studying soil-reinforcement interactions in cold climates. Integrating geosynthetics, such as geocells, into a hypoplastic framework under freeze-thaw cycles enables a deeper understanding of soil-geocell behavior in these conditions.

This study aims to evaluate geosynthetics-soil interactions in cold regions, focusing on geocell-reinforced soils under freeze-thaw cycles. We extend the hypoplastic constitutive model with intergranular strain considerations to simulate the mechanical behavior of frozen and unfrozen soils. A temperature-dependent state parameter accounts for freezing effects on stiffness, strength, and strain. Through triaxial testing and numerical validation with 131 Sand, the study assesses geocell reinforcement performance under various environmental and loading conditions, contributing to safer, more resilient geotechnical infrastructure in cold climates.

2. Soil constitutive model

The Hypoplastic constitutive model is widely used to describe the nonlinear, incremental stress-strain behavior of soils without invoking yield surfaces or plastic potentials. It models the stress rate as a function of the current stress state, void ratio, and strain rate, as shown in [25]:

$$\dot{T}^u = F(T, e, D) \tag{1}$$

This equation defines the evolution of stress in unfrozen soil under the influence of the stretching tensor D, current stress tensor T, and void ratio e. To interpret the stress state, the stress tensor T is decomposed into scalar invariants: mean stress p, deviatoric stress q, and a load-angle-based parameter z, as follows [26]:

$$T = [p = tr \, \sigma/3, \quad q = \sqrt{\frac{3}{2}tr \, \sigma^2}, \quad z = sin(3\theta)] \tag{2}$$

These components allow the stress state to be expressed in a simplified but physically meaningful way for constitutive modeling. The total strain tensor for unfrozen soil is also broken down into volumetric and deviatoric components:

$$\varepsilon_{\text{total}}^{u} = \left[\varepsilon_{\text{v}}^{u} = \text{tr } \varepsilon, \quad \varepsilon_{\text{s}} = \sqrt{\frac{2}{3} \text{ tr } \varepsilon^{2}} \right]$$
(3)

This separation helps distinguish between compaction/swelling and shear deformation behavior. The function F in Eq. (1) is further developed to account for both stiffness and density contributions to the material response, and their directional dependence on loading paths [25]:

$$F = f_s^{u}(tr T, e) \left(L\left(\frac{T}{tr T}, D\right) + f_d^{u}(tr T, e) N\left(\frac{T}{tr T}\right) ||D|| \right)$$
(4)

Here, f_s^u is the stiffness factor, and f_d^u is the density factor, both of which evolve with stress and void ratio. Functions L and N define material behavior under loading and unloading conditions. The density factor f_d^u is defined using void ratio parameters that reflect soil compaction limits [25]:

$$f_d^{\ u} = \left(\frac{e - e_d}{e_c - e_d}\right)^{\alpha} \tag{5}$$

This formulation expresses how the stiffness is influenced by how close the soil is to its critical or dense states, using parameter α . The stiffness factor f_s^u incorporates parameters related to soil fabric and confining pressure [25]:

$$f_{s}^{u} = \frac{\frac{h_{s}}{n} \left(\frac{e_{i}}{e_{i}}\right)^{\beta} \frac{1+e_{i}}{e_{i}} \left(\frac{3p}{h_{s}}\right)^{1-n}}{3+a^{2}-\sqrt{3}a \left(\frac{e_{i0}-e_{d0}}{e_{c0}-e_{d0}}\right)^{\alpha}}$$

$$\tag{6}$$

This complex equation captures the nonlinear stiffness evolution with pressure, void ratio, and soil fabric constants, including granular hardness h_s , exponent nnn, and shape factor a. The shape factor a links the stiffness to the critical friction angle ϕ_c [25]:

$$a = \frac{\sqrt{3}(3 - \sin\phi_c)}{2\sqrt{2}\sin\phi_c} \tag{7}$$

To improve the Hypoplastic model's realism under cyclic or complex loading, inter-granular strain effects are included using stress-rate tensors M and H [26]:

$$\begin{cases} M = m_T \rho^{\chi} L + m_R (1 - \rho^{\chi}) L + \rho^{\chi} (m_T + m_R) L \, \delta \, \operatorname{tr} \, \delta, & \delta : D \leq 0 \\ H = 1 \\ M = m_T \rho^{\chi} L + m_R (1 - \rho^{\chi}) L + \rho^{\chi} (1 + m_T) L \, \delta \, \operatorname{tr} \, \delta - \rho^{\chi} N \delta, & \delta : D > 0 \end{cases}$$

$$H = 1 - \rho^{\beta r} \delta \, \operatorname{tr} \, \delta$$

$$(9)$$

This complex relationship defines how the internal strain tensor δ evolves with loading, controlled by normalized strain $\rho = \frac{\|\delta\|}{R}$, where R is a material-specific reference value. Parameters m_R , m_T , β_r , R and χ must be calibrated to fit lab data. To account for temperature-dependent mechanical changes in frozen soils, Yu et al. [27] introduced a temperature-state function b(t):

$$0 \le b(t) = exp(\frac{t_{min} - t}{t_f - t}) \le 1, \ t_{min} \le t < t_f$$
 (10)

This dimensionless parameter decreases with falling temperature, representing reduced mobility and strength due to ice formation. Using b(t), the volumetric ice fraction S_i can be modeled as [27]:

$$S_i = \frac{ice \, volume}{pore \, volume} \tag{11}$$

$$S_i(b) = \xi b^k \tag{12}$$

Where ξ indicates the portion of freezable water (equal to 1 for coarse soils), and k controls how fast the ice fraction grows as temperature drops. To model frozen soils, the strain tensor is extended by adding terms to account for ice formation and water migration during freezing [27]:

$$\varepsilon_{total}^{f} = \left[\varepsilon_{v}^{f} = \varepsilon_{v}^{u} + \varepsilon_{t}^{w} + \varepsilon_{t}^{p}, \quad \varepsilon_{s} = \sqrt{\frac{2}{3} \operatorname{tr} \varepsilon^{2}}\right]$$
(13)

This new strain formulation captures the expansion and redistribution caused by phase changes. The strain due to water migration is [27]:

$$\varepsilon_t^{\ W} = b_2 u_w \frac{\partial t}{\partial x_i} dt \tag{14}$$

Where u_w is a migration potential driven by temperature gradients, and b_2 is an empirical constant. The strain from water-to-ice phase change is given by [27]:

$$\varepsilon_t^p = \frac{\rho_w - \rho_i}{(1 - S_i)\rho_w + S_i \rho_i} [S_i \varepsilon_t^w + (1 - S_i)t] \tag{15}$$

This captures the increase in soil volume due to ice expansion, adjusted by ice fraction S_i . The frozen critical friction angle evolves with temperature through ice content:

$$\varphi_c{}^f = \frac{\xi \varphi_c{}^u b^k}{c_1} \tag{16}$$

This relationship helps adjust the mechanical response of frozen soils in the stiffness matrix. Void ratio parameters also change with freezing:

$$e^f = e\left(1 + \frac{\xi b^k}{c_2}\right) \tag{17}$$

Here, c_2 is a calibration factor that adjusts the volumetric change due to ice formation. Finally, the granular hardness adjustment due to confining pressure follows Bauer's relationship [25]:

$$\frac{e_i}{e_{i0}} = \frac{e_c}{e_{c0}} = \frac{e_d}{e_{d0}} = exp\left[-\left(\frac{3p}{h_s}\right)^n\right] \tag{18}$$

This equation captures how stiffness changes with pressure and void ratio reduction in frozen soils. To evaluate and calibrate the predictive capability of the proposed extended hypoplastic model, a series of drained triaxial compression tests were conducted on frozen 131 Sand under carefully controlled laboratory conditions. The calibration process was essential to determine the model parameters that best replicate the observed stress–strain and volumetric behavior of the material under freezing conditions. Sand specimens were prepared by dry pluviation in three layers into standard triaxial molds, with each layer compacted to achieve a uniform relative density of 60%. The samples were then vacuum saturated to ensure full saturation, a critical condition for ice formation during the freezing phase. Specimens were frozen at -10 °C for seven days to allow complete and uniform freezing. After freezing, each sample was

tested under confining pressures of 100 and 200 kPa, with axial loading applied at a constant displacement rate of 1 mm/min. Both axial and volumetric strains were recorded throughout the tests.

The calibration of the hypoplastic model was conducted using a combination of literature-based data and laboratory testing. Initially, model parameters for unfrozen 131 Sand—such as granular stiffness, critical state friction angle, and void ratio limits—were adopted from established literature and prior studies on similar sandy soils. These unfrozen parameters were then input into the extended hypoplastic model, which incorporates temperature-dependent formulations to simulate the effects of freezing, including ice formation and thermal strain. By applying the temperature-state function and associated modifications within the model, updated soil parameters for frozen conditions were generated. These frozen-state parameters inherently accounted for reductions in mobility, increases in apparent cohesion, and changes in void ratio and friction angle due to ice bonding. The model outputs using these updated parameters were then compared with the results of drained triaxial compression tests on frozen 131 Sand. The comparison showed strong agreement in both stress-strain and volumetric strain responses, confirming the reliability of the extended model and the suitability of the derived parameters for representing frozen soil behavior. The calibration was conducted in multiple iterations, with each set of parameters evaluated by comparing model predictions to experimental data under both confining pressures. As illustrated in Fig. 1, the model successfully reproduced the nonlinear stress-strain response and volumetric strain behavior of frozen 131 Sand, confirming the robustness and validity of the calibration procedure for use in further numerical simulations involving geocell pullout.

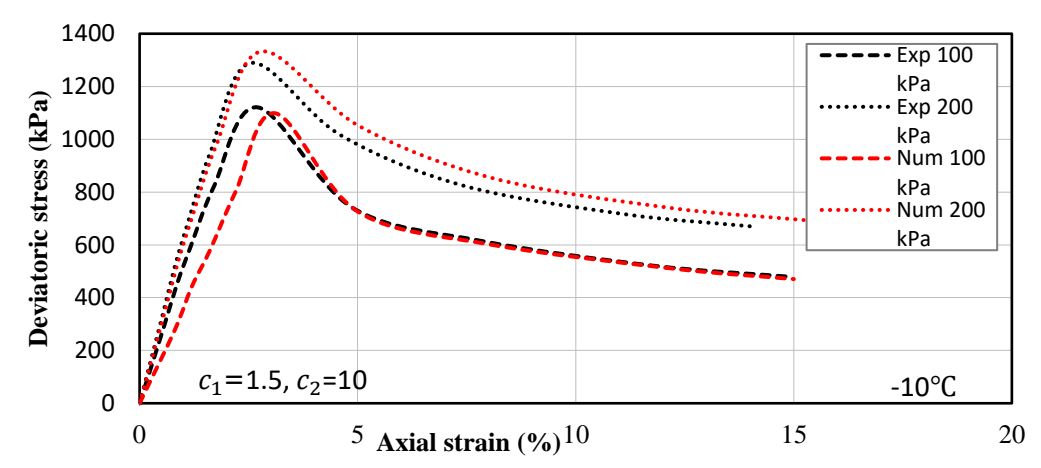


Fig. 1. Comparison between experimental tests and proposed model results for frozen.

3. FEM modeling

The mechanical behavior of geocell-reinforced soil was investigated using a pullout box model simulated in Plaxis 3D, a finite element software widely used for advanced geotechnical analyses. The experiments utilized a large pullout apparatus with a box measuring 90 cm in length, 50 cm in width, and 50 cm in depth. Normal pressure was applied using an airbag, delivering a maximum pressure of 75 kPa. The geocell layer, with dimensions of 80 cm in length and 40 cm in width, was placed within the apparatusThe aim of this numerical study was to simulate the interaction between the geocell reinforcement and the surrounding soil, particularly under conditions involving freeze—thaw cycles. In the Plaxis 3D environment, the pullout box was modeled with dimensions large enough to minimize boundary effects, based on recommendations from prior literature and preliminary mesh sensitivity analyses. The geocell layer was modeled using geogrid elements, which are available in Plaxis as embedded structures that resist axial tensile forces. These elements were configured to replicate a diamond-shaped geocell pattern, equivalent to the behavior of biaxial geocells. In Plaxis 3D, the geocell was modeled using embedded geogrid elements, which are designed to capture the interaction between

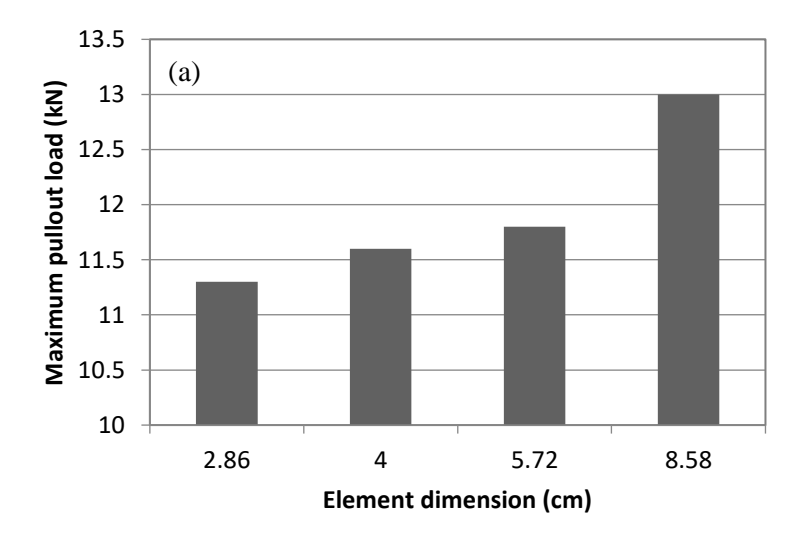
reinforcement and surrounding soil through a node-based formulation. The software evaluates relative displacements between the geogrid and adjacent soil at nodal points along the geogrid elements. Based on these relative movements, axial forces are mobilized in the geogrid and transferred to the surrounding soil. This formulation inherently accounts for the load transfer mechanisms and bond-slip behavior along the geocell—soil interface, without requiring explicit interface elements. As a result, the model can realistically simulate the mechanical response of the geocell reinforcement under different loading and thermal conditions.

The geogrid was defined as a linearly elastic isotropic material, with mechanical properties derived from experimental studies (see Table 1). No failure criteria were applied to the geogrid, assuming the reinforcement does not fail under the loading conditions used in this simulation. The soil-geogrid interaction was modeled using the embedded beam feature in Plaxis 3D, which allows for defining interface strength parameters between the geogrid and the surrounding soil. To replicate realistic interaction behavior, a reduction factor of 2/3 was applied to the interface strength in the horizontal direction, as suggested by Leshchinsky and Ling [28]. This factor accounts for the partial shear transfer between the geocell walls and the infill material under vertical loading. The soil medium used in the simulation was 131 Sand, modeled using an extended hypoplastic constitutive model that accounts for the complex stress-strain behavior of granular materials under freeze-thaw conditions. The hypoplastic parameters of this have been evaluated by Namaei et al [29] and presented in Table 2. This advanced model captures the nonlinear, path-dependent response of soil more accurately than conventional models, making it well-suited for simulating the effects of cyclic freezing and thawing on soil-structure interaction. The hypoplastic parameters used in the model were calibrated through laboratory experiments on frozen and unfrozen 131 Sand with 60 % relative density, ensuring consistency between numerical and physical behavior. Key input properties, such as initial void ratio, granular skeleton stiffness, critical state parameters, and intergranular strain coefficients, were derived based on these experimental results and validated using drained triaxial tests. In Plaxis 3D, the geocell-reinforced pullout box was discretized with a medium-density mesh, ensuring a balance between computational efficiency and accuracy, particularly near the geocell-soil interfaces where stress gradients are high. A finer mesh was applied selectively in the vicinity of the reinforcement to capture localized interaction effects. A sensitive analysis was performed in order to choose meshing elements size, very fine, fine, medium and coarse element distribution with element dimension 2.86, 4, 5.72 and 8.58 cm were adopted as the element distribution, respectively. The maximum pullout force obtained from these four models is shown in Fig. 2(a). It can be seen that the element dimension lower than 5.72 cm didn't affect the value of maximum pullout force significantly. Hence, the medium element distribution with 5.72 cm element dimension was chosen as the mesh size of this simulation to consider both the analyses time and the accuracy of the result. The simulation setup provided a realistic framework for evaluating load transfer mechanisms and the effectiveness of geocell reinforcement under varying thermal and mechanical loading conditions. To accurately replicate laboratory conditions and eliminate artificial boundary effects, carefully selected boundary constraints were applied to the model:

- Bottom Boundary: The entire bottom surface of the soil domain was fixed in all directions (Ux = Uy = Uz = 0), representing a rigid base condition and preventing any movement of the lower boundary.
- Lateral Boundaries (Vertical Side Faces):
 - X- and Y-Direction Constraints: The vertical side faces of the model were constrained in the horizontal directions perpendicular to each boundary face. That is, the X-direction was fixed on the YZ-planes, and the Y-direction was fixed on the XZ-planes.
 - o Z-Direction Freedom: Vertical (Z) movement was allowed on the side boundaries to simulate realistic vertical stress distribution and to avoid over-constraining the model.

- Top Boundary (Soil Surface): The top surface of the soil remained *free* in all directions to simulate realistic surface conditions. Vertical *surcharge pressures of 20 kPa and 60 kPa* were applied to this surface to replicate field loading conditions. These loads were applied over the entire top surface using a uniform pressure boundary condition.
- Geocell Displacement Condition: To simulate the pullout process, a *prescribed horizontal displacement of 1 mm* was applied to the geocell elements in the direction of extraction. This was done incrementally to monitor the evolution of pullout force and load transfer mechanisms.

This boundary configuration effectively isolated the pullout response of the geocell from any unrealistic constraints and provided a reliable representation of the field-scale behavior within a controlled simulation domain. By fixing horizontal movement on lateral faces and allowing vertical movement on all but the bottom surface, the model preserved realistic deformation modes while preventing lateral expansion that does not occur in the confined laboratory setup. This numerical approach allowed for a detailed investigation of load transfer mechanisms, confinement effects, and the overall reinforcement performance of the geocell under different loading and thermal conditions. The final model is demonstrated in Fig. 2(b).



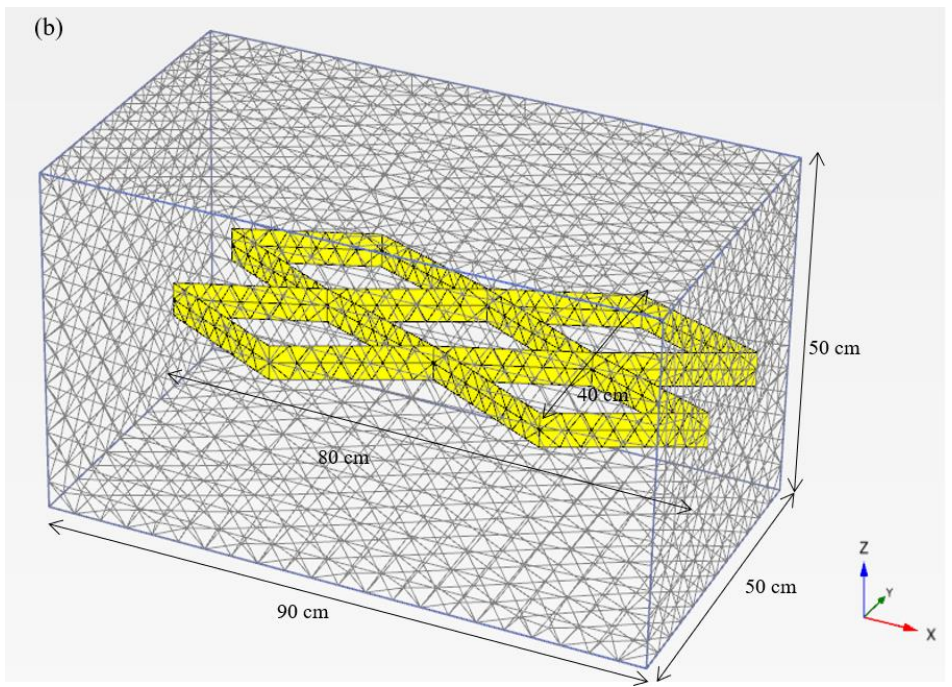


Fig. 2. Numerical modeling of pullout test; (a) mesh size effect; (b) simulated geocell pullout test after meshing.

Table 1. BX geocell input parameters [30].

Table 10 211 govern input parameters [5 v].									
Secant modulus at 10 % strain level (kN/m)	125								
Secant modulus at 5 % strain level (kN/m)	160								
Ultimate tensile strength (kN/m)	20								
Height (mm)	100								
Aperture size $(cm \times cm)$	25 × 25								

Table 2. Soil hypoplastic parameters [29].

Parameter	$arphi_c$	n	$h_s(kPa)$	e_{do}	e_{c0}	e_{io}	α	β	m_R	m_t	R	eta_r	χ
Value	38.4	0.26	460000	0.41	0.82	0.98	0.3	1.5	3.5	1.5	7E-5	0.7	0.8

To simulate freeze—thaw (FT) cycles within Plaxis 3D, a temperature-dependent hypoplastic constitutive model was implemented through a user-defined soil model subroutine. The FT process was modeled by alternating the temperature input between +10 °C (thawing phase) and -10 °C (freezing phase). For each thermal stage, the hypoplastic input parameters—such as critical state friction angle, granular stiffness, void ratio parameters, and intergranular strain coefficients—were recalculated based on the corresponding temperature. These updated parameters were manually assigned at the beginning of each phase to capture the evolving mechanical behavior of the soil under thermal cycling. In this study, three full freeze—thaw cycles were simulated to investigate the progressive degradation of geocell pullout resistance. This approach allowed for realistic modeling of soil behavior under repeated thermal loading, including changes in stiffness, strength, and interface performance due to ice formation and melting.

4. Verification

In order to verify the numerical analysis, a series of monotonic and multistage geocell pullout tests were performed. A pullout apparatus with a large box with 90 cm length, 50 cm width and 50 cm depth was used. Normal pressure was applied by the use of an airbag which applied 75 kPa maximum pressure. The pullout force was applied by 2.5 ton hydraulic jack with the facility to apply 75 mm maximum displacement and up to 100 Hz frequency. A view of apparatus is illustrated in Fig. 3. To prepare poorly graded sand and geocell, primarily the sandy materials were placed in the lower part of the apparatus in three layers of 7.5 cm to reach 22.5 cm height. According to the practical problems, each soil layers are compacted with electrical hammer and reach relative densities more than 70 %. In this study, the relative densities of the soil samples were kept constant and equal to 70 % in all tests. Subsequently, the geocell layer with 80 cm length and 40 cm width was placed at the reached level. The geocells were compounded of various Polyethylenes and additives. Polyethylene strips were ultrasonically welded to other strip at specific distance intervals. Fig. 4 illustrated geocell placement in the box.



Fig. 3. Pullout test apparatus.



Fig. 4. Geocell placement in pullout box.

Fig. 5 illustrates the numerical and experimental results of monotonic pullout load versus displacement under 20 and 60 kPa surcharge. It can be seen in Fig. 5 that the monotonic ultimate pullout load was predicted well. Also, the geocell pullout load – displacement trend was successfully captured which shows the verification of the numerical modeling.

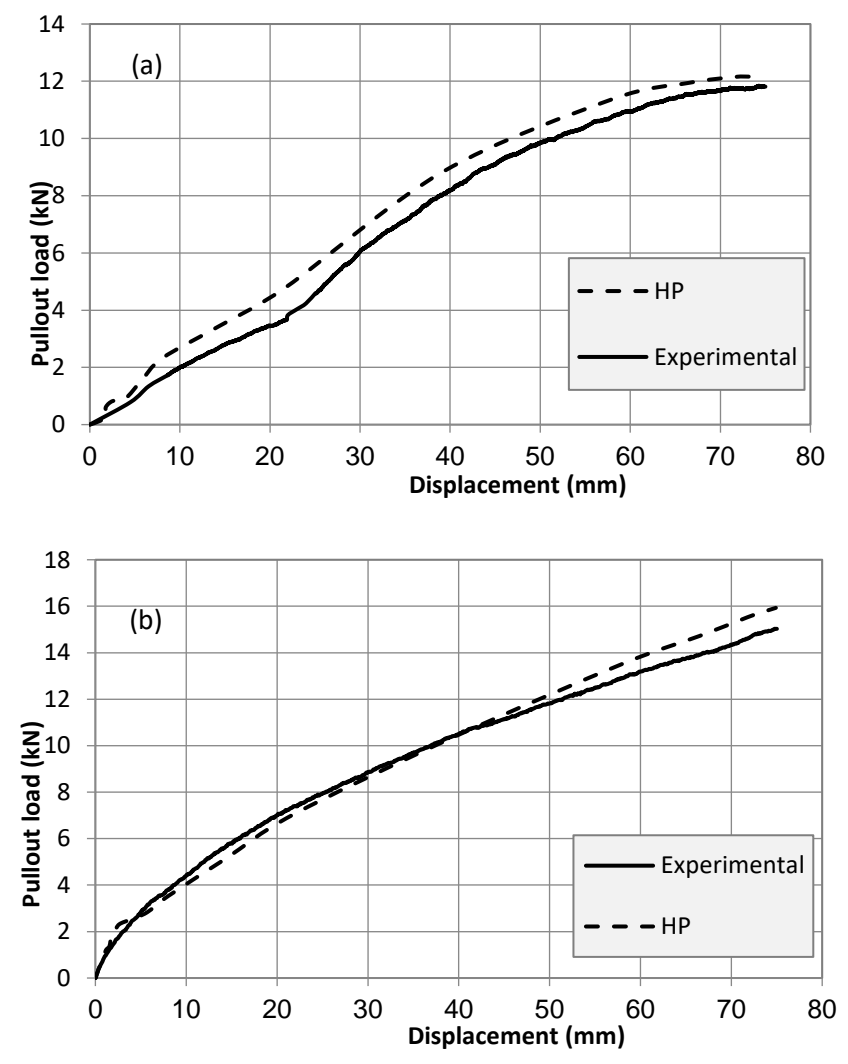


Fig. 5. Monotonic pullout behavior of geocell: (a) 20 kPa vertical pressure; (b) 60 kPa vertical pressure.

5. Results and dicussion

To investigate the behavior of geocell-reinforced soil under different thermal conditions, a series of pullout simulations were conducted in Plaxis 3D, focusing on the comparison between frozen and unfrozen states. The pullout tests simulate the extraction of a geocell-reinforced layer embedded in 131 Sand under controlled boundary conditions, mimicking field-scale pullout behavior influenced by seasonal freezing and thawing. Fig. 6 shows the results of the displacement and load–displacement response under both thermal scenarios. The numerical results demonstrated significant differences in pullout resistance and displacement characteristics between the frozen and unfrozen conditions. In the unfrozen state, the geocell reinforcement exhibited a lower pullout resistance, with larger displacements observed near the geocell interface. This behavior is attributed to the reduced shear strength and cohesion of granular soil in its unfrozen form, allowing easier relative movement between the reinforcement and the surrounding soil. Conversely, in the frozen condition, the pullout resistance increased substantially, and the displacement along the reinforcement was significantly reduced. This improvement in performance is primarily due to the formation of ice bonds within the soil matrix, which act as temporary cementing agents that enhance inter-particle connectivity and increase effective soil cohesion. The enhanced pullout behavior in the frozen state is governed by several key mechanisms:

- 1. Microstructural Bonding: The freezing process induces the formation of a rigid ice structure within the soil pores, which binds particles together and creates a stiffer medium that resists deformation.
- 2. Increased Interface Shear Strength: The ice-enforced soil matrix improves the shear strength at the geocell—soil interface, requiring higher forces to mobilize pullout failure.
- 3. Reduced Deformability: The frozen soil exhibits higher stiffness, distributing the applied pullout force over a broader area and mitigating local deformation.
- 4. Diminished Pore Pressure Effects: With water transformed into ice, pore water pressure drops, reducing the potential for soil softening and slippage at the interface.

The results confirm that freezing substantially enhances the mechanical interaction between geocell reinforcement and soil, increasing pullout resistance and reducing deformation under loading. These findings highlight the importance of accounting for thermal effects in geotechnical design, especially in cold regions.

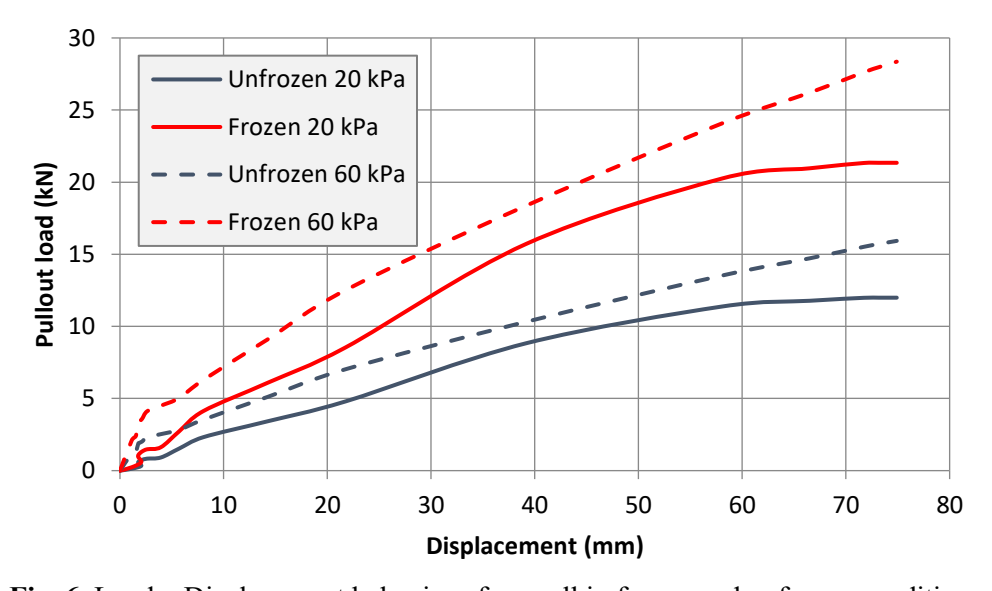


Fig. 6. Load – Displacement behavior of geocell in frozen and unfrozen conditions.

The pullout capacity of geocell-reinforced 131 Sand was numerically evaluated using Plaxis 3D under both frozen and unfrozen conditions and the results are demonstrated in Fig. 7. The analysis clearly demonstrated a significant enhancement in pullout resistance in the frozen state. In the unfrozen condition, the maximum pullout force was approximately 11.9 kN under 20 kPa, which is consistent with typical values observed in dry or saturated sandy soils with moderate confinement. The load–displacement curve showed a gradual increase to peak load, followed by a drop in resistance, indicating slippage between the geocell and soil due to low interface bonding strength. In contrast, under frozen conditions, the maximum pullout force increased substantially to around 21.2 kN, representing a 78% increase compared to the unfrozen state. The same behavior can be seen under 60 kPa surcharge pressure. The frozen soil exhibited a stiffer response with a steeper load–displacement curve, a higher peak force, and significantly less post-peak deformation. This improvement is attributed to the formation of ice bonds within the soil structure and at the geocell–soil interface. Key factors contributing to the enhanced pullout capacity in frozen soil include:

- Ice Bonding: The transformation of pore water into ice increases cohesion and restricts particle movement
- Higher Interface Strength: Ice bonds increase resistance at the geocell-soil interface, delaying pullout initiation.
- Greater Stiffness and Confinement: The frozen soil mass provides higher lateral resistance and distributes loads more evenly.

These findings demonstrate that frozen conditions significantly enhance the pullout performance of geocell-reinforced systems, especially relevant for engineering applications in cold regions.

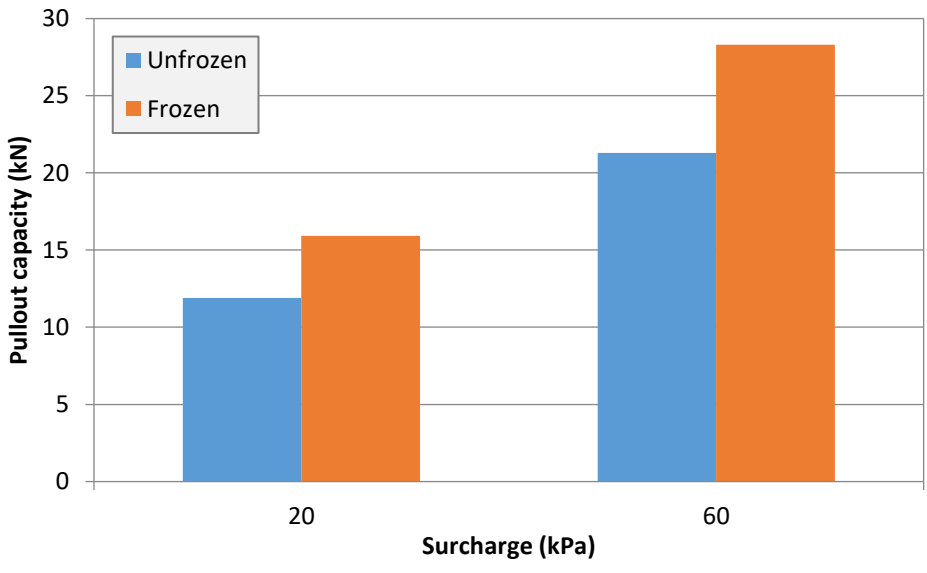


Fig. 7. Pullout capacity of geocell in frozen and unfrozen soil.

To investigate the effect of freeze-thaw (FT) cycles on the pullout resistance of geocell reinforcements, a series of numerical simulations were performed using the proposed 3D model, in which the temperature was varied cyclically between +10 °C and -10 °C to simulate realistic seasonal freezing and thawing conditions. These temperature variations were applied to the geocell-soil system to replicate the thermal stresses and structural changes that occur in cold climate environments, particularly in areas subject to repeated freeze-thaw phenomena. Fig. 8 presents the results of geocell pullout tests conducted under a uniform surcharge pressure of 60 kPa, after being subjected to one (FT1), two (FT2), and three (FT3) freeze-thaw cycles. The figure illustrates the relationship between pullout force (kN) and displacement

(mm), providing a comparative understanding of how repeated thermal cycling influences the geocell's resistance performance. As observed, the pullout resistance of the geocell significantly decreases with the increasing number of freeze-thaw cycles. After the first cycle (FT1), the maximum pullout force reached approximately 28.3 kN, indicating strong interaction between the geocell walls and the surrounding soil. However, following the second (FT2) and third (FT3) cycles, the maximum resistance dropped to about 26.4 kN and 24.0 kN, respectively. This reduction highlights the progressive degradation of the interfacial shear strength and soil confinement efficiency. The observed decline in pullout performance is primarily attributed to microstructural changes in the soil, including the formation and melting of ice lenses, pore expansion, disruption of particle bonding, and a loss of confining pressure around the geocell walls during thawing. These phenomena reduce the effective stress and compromise the integrity of the geocell-soil interface, leading to a diminished load transfer mechanism. In conclusion, Fig. 8 demonstrates the critical role that freeze-thaw cycles play in reducing the mechanical effectiveness of geocell reinforcements in cold climates. The results underscore the importance of accounting for thermal effects in the design and durability assessment of geosynthetic-reinforced soil systems deployed in frost-susceptible regions.

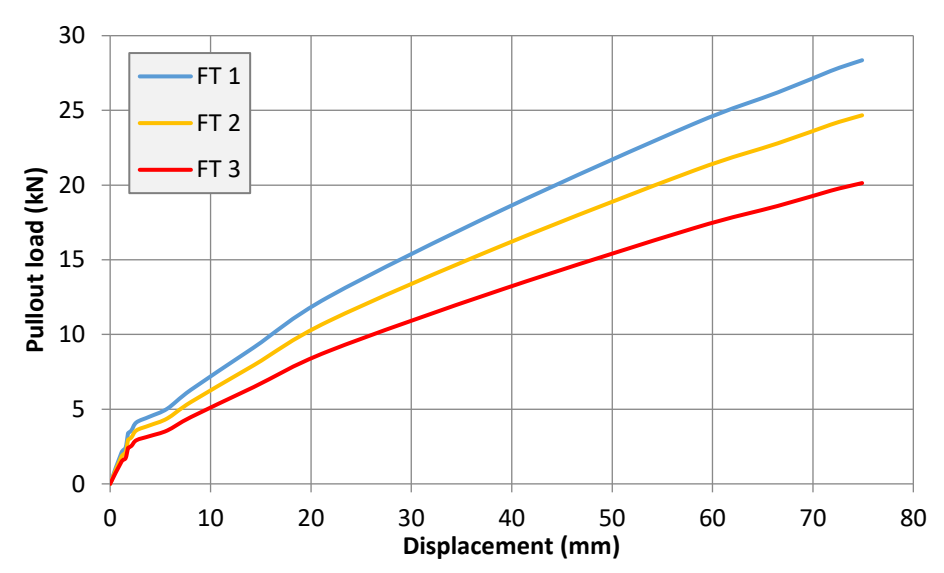


Fig. 8. Effect of freeze-thaw cycles on geocell pullout resistance.

6. Conclusions

This study demonstrates the efficacy of an extended hypoplastic constitutive model in accurately modeling the behavior of geocell-reinforced 131 Sand under diverse thermal conditions, including frozen, unfrozen, and freeze-thaw (FT) cycles. Built on its original design to capture the nonlinear, incremental stress—strain behavior of granular materials without yield surfaces, the model was advanced with temperature-dependent features—such as a temperature-state function, adjusted void ratio parameters, and a critical state friction angle modified by ice content—to simulate phase transitions and structural changes in frozen soils effectively.

Validation through drained triaxial compression tests on frozen 131 Sand at 100 and 200 kPa confining pressures showed strong agreement between model predictions and experimental data, successfully replicating nonlinear stress–strain relationships and volumetric deformations. This validation confirms the model's robustness for frozen soil simulations and its suitability for integration into large-scale numerical analyses, such as geocell pullout studies.

Using this validated model, 3D pullout simulations in Plaxis 3D revealed the profound impact of thermal states on geocell performance: frozen conditions increased pullout resistance by 78% compared to unfrozen states due to ice bond formation, which enhances cohesion and limits soil-reinforcement movement; unfrozen conditions exhibited greater deformation and lower resistance due to weaker

interface bonding; and FT cycles reduced pullout capacity by approximately 15% after three cycles, reflecting degradation from ice melting, particle rearrangement, and diminished confinement. These results emphasize the critical role of thermal effects in designing geosynthetic-reinforced structures in cold regions.

The extended hypoplastic model provides a reliable framework for predicting geocell behavior across various thermal conditions, offering a valuable tool for optimizing reinforcement systems in frost-susceptible environments. By addressing seasonal temperature variations that influence soil-structure interactions, this study supports the development of more resilient geotechnical infrastructure in cold climates.

One limitation of this study is that while the sandy soil was assumed to be fully saturated prior to freezing—a condition representative of natural cold-region environments—the formation of ice lenses was not explicitly modeled. The mechanical simulations were carried out under drained conditions, focusing on the stress—strain response and pullout behavior rather than pore pressure dynamics or frost heave. Although the temperature-dependent hypoplastic model captures the mechanical effects of ice bonding and increased stiffness, it does not simulate water migration or segregated ice growth. As such, the localized effects of ice lens formation around the geocell, which may influence confinement and load transfer mechanisms, are not considered in this analysis. Future research involving coupled hydrothermal-mechanical modeling is recommended to address these phenomena more comprehensively.

Funding

This research is supported by the research grant of the Imam Khomeini International University (Number: 259684)

Conflicts of interest

The authors declare that they have no known competing financial interests or personal relationships that could have appeared to influence the work reported in this paper.

Authors contribution statement

Ali Namaei-Kohal: Data curation; Formal analysis; Investigation; Methodology; Resources; Software; Writing – original draft.

Alireza Ardakani: Project administration; Supervision; Review & editing.

References

- [1] Li, K.Q., Yin, Z.Y., Qi, J.L., & Liu Y. State of the art: Constitutive modeling of frozen soils. Arch Comput Methods Eng 2024;31:3801–42.
- [2] Nishimura, S., Gens, A., Olivella, S., & Jardine R. THM coupled finite element analysis of frozen soil: formulation and application. Geotechnique 2009;59:159–71.
- [3] Yang, Y., Lai, Y., Dong, Y., & Li S. The strength criterion and elastoplastic constitutive model of frozen soil under high confining pressures. Cold Reg Sci Technol 2010;60:154–60.
- [4] Yao, X., Qi, J., Liu, M., & Yu F. A frozen soil creep model with strength attenuationA frozen soil creep model with strength attenuation. Acta Geotech 2017;12:1385–93.
- [5] Hou, F., Lai, Y., Liu, E., Luo, H., & Liu X. A creep constitutive model for frozen soils with different contents of coarse grains. Cold Reg Sci Technol 2018;145:119–26.
- [6] Li, D., Zhang, C., & Ding G. Fractional derivative-based creep constitutive model of deep artificial frozen soil. Cold Reg Sci Technol 2020;170.

- [7] He, J., Niu, F., Jiang, H., & Jiao C. Fractional viscoelastic-plastic constitutive model for frozen soil based on microcosmic damage mechanism. Mech Mater 2023.
- [8] Xu, G., Wu, W., & Qi J. An extended hypoplastic constitutive model for frozen sand. Soils Found 2016;56:704–11.
- [9] Xu, G., Wu, W., & Qi J. Modeling the viscous behavior of frozen soil with hypoplasticity. Int J Numer Anal Methods Geomech 2016;40:2061–73.
- [10] Xu, X., Wang, Y., Yin, Z., & Zhang H. Effect of temperature and strain rate on mechanical characteristics and constitutive model of frozen Helin loess. Cold Reg Sci Technol 2017;136:44–51.
- [11] Mohammadi, B.H., & Ardakani A. Numerical prediction of circular tunnel seismic behavior using hypoplastic soil constitutive model. Int J Geotech Eng 2018:1–14.
- [12] Mohammadi, B.H., & Ardakani A. Calibration of hypoplastic constitutive model with elastic strain range for Firoozkuh sand. Geotech Geol Eng 2020;38:5279–93.
- [13] Latha, G.M., Dash, S.K., and Rajagopal, K. ''Equivalent continuum simulations of geocell reinforced sand beds supporting strip footings. Geotech Geol Eng 2008;26:387–98.
- [14] Khedkar, M., & Mandal J. Pullout response of cellular reinforcement under low normal pressure. Int Journal Geotech Eng 2013;3:75–87.
- [15] Biabani, M.M., Indraratna, B., and Ngo NT. 'Modeling of geocell reinforced sub ballast subjected to cyclic loading. Geotextile Geomembr 2016;44:489–503.
- [16] Tavakoli, G.T.M, and Motarjemi F. 'Interfacial properties of geocell reinforced granular soils. Geotextile Geomembr 2018;46:384–95.
- [17] Fakharian, K., & Pilban A. Pullout tests on diagonally enhanced geocells embedded in sand to improve load-deformation response subjected to significant planar tensile loads. Geotextile Geomembr 2021;49:1229–44.
- [18] Namaei-kohal, A., Ardakani, A., & Hassanlourad M. Cyclic and post-cyclic geocell pullout behavior in cohesionless soi. Sci Iran 2023:1–36.
- [19] Li, C., Vennapusa, P.K.R., Ashlock, J., & White DJ. Mechanistic-based comparisons for freeze-thaw performance of stabilized unpaved roads. Cold Reg Sci Technol 2017;141:97–108.
- [20] Cui, F., Xiao, C., Han, J., Gao, S., & Tian W. Performance of laboratory geogrid-reinforced retaining walls under freeze-thaw cycles. Geosynth Int 2022;29:81–98.
- [21] Fattah MA and MY. Assessment of two nearby interfering strip footings of different embedment depths in saturated cohesive soils. Mag Civ Eng 2024;14:149.
- [22] Fattah, M. Y., Al-Haddad,, L.A., Mo'men Ayasrah, Jaber, A., and SA-H. Coupled Finite Element and Artificial Neural Network Analysis of Interfering Strip Footings in Saturated Cohesive Soils. Transp Infrastruct Geotechnol 2024;11:2168–85.
- [23] Ayasrah, M., & Fattah MY. 3D numerical response of different pipe pile under combined loadings condition embedded in loose sand. Int J Geotech Eng 2024;18:702–718.
- [24] Fattah MA and MY. Finite Element Analysis of Two Nearby Interfering Strip Footings Embedded in Saturated Cohesive Soils. Civ Eng J 2023;9:1–18.
- [25] Bauer E. Calibration of comprehensive hypoplastiv model for granular materials. Soils Found 1996;36:13–26.
- [26] Niemunis, A., & Herle I. Hypoplastic model for cohesionless soils with elastic strain range. Mech Cohesive-Frictional Mater 1997;2:279–99.
- [27] Yu, F., Guo, P., & Na S. A framework for constructing elastoplastic constitutive models for frozen and unfrozen soils. Int J Numer Anal Methods Geomech 2022;46:436–66.
- [28] Leshchinsky, B., and Ling, H.I. 'Effects of geocell confinement on strength and deformation behavior of gravel. J Geotech Geoenvironmental Eng 2013;139:340–52.
- [29] Namaei-kohal, A. Ardakani, A., and Hassanlourad M. 'Hypolastic Soil Model Parameters calibration For Tehran Silica Sand and Verification with a Monotonic Geocell Pullout Test. Arab J Geosci 2022;15:824-837.
- [30] Ardakani, A., and Namaei A. 'Numerical Investigation of Geocell Reinforced Slopes Behavior by considering Geocell Geometry Effect. Geomech Eng 2021;24:589–97.